A GIS tool for the land carrying capacity of large solar plants

Available online at www.sciencedirect.com

ScienceDirect

Energy Procedia 48 (2014) 1576 – 1585

Energy Procedia

SHC 2013, International Conference on Solar Heating and Cooling for Buildings and Industry
September 23-25, 2013, Freiburg, Germany

A GIS tool for the land carrying capacity of large solar plants

Enrico Borgogno Mondino[a], Enrico Fabrizio[a,]*, Roberto Chiabrando[b]

[a]*University of Torino, DISAFA, Grugliasco (TO) 10095, Italy*
[b]*University of Torino, DIST, Torino 10127, Italy*

Abstract

A tool for the estimation of the land carrying capacity of large solar plants, such as ground-mounted PV plants or solar thermal plants, is developed in GIS environment. The scope is to verify to what extent the constraints that governments and authorities have imposed on the construction of new large ground-mounted soalr plants affect the future developments of PV. The tool is applied to a large study area of North-Italy and specifically to solar photovoltaic plants but the results can be easily generalized to include large solar thermal plants. The peculiarity of the tool development is that both qualitative and quantitative criteria are merged together in order to obtain the final indicator, and that the weight of the objective function are estimated by means of an ANN. The available area are very limited and strongly influenced by the normative qualitative criteria (restricted areas).

Selection and peer review by the scientific conference committee of SHC 2013 under responsibility of PSE AG

Keywords: Land use; photovoltaic; carrying capacity; GIS

1. Introduction

The application of geomatics to the assessment of renewable resources, in particular to the solar resource [1], is a topic worth to be investigated. For an up-to-date review see Calvert [2]. Energy resources are spatially distributed and GIS can manage georeferenced information about them in order to assess the technical and economical feasibility of the source exploitation [3,4] linking the information on the source itself with other types of georeferenced information such as population, existing networks, etc. Moreover, GIS can also be used to create site

* Corresponding author. Tel.: +39-(0)11-670-5525; fax: +39-(0)11-670-5516.
E-mail address: enrico.fabrizio@unito.it

1876-6102
Selection and peer review by the scientific conference committee of SHC 2013 under responsibility of PSE AG
doi:10.1016/j.egypro.2014.02.178

selection support systems as it is performed in many other fields [5,6]. In this paper, GIS is applied in order to identify and quantify the areas that are suitable for the installation of ground-mounted PV plants through the aggregation of qualitative and quantitative criteria into a final indicator. Studies of the same authors that concentrated on the assessment of the territorial [7] and visual impact [8] of large solar plants as ground-mounted PV plants were previously performed. The areas are also classified as a function of the suitability of the installation of PV plants based on criteria such as solar radiation, temperature profiles and annual rainfall. The estimation of the weights to be assigned to each criterion in the objective function is done by means of an Artificial Neural Network (ANN) that was trained with data from observed existing PV plants.

Nomenclature

B	Boolean operator of exclusion/inclusion criterion
C	quantification criterion
f	objective function
s	slope
x,y	land unit coordinates
α	weight
γ	orientation (azimuth, expressed in degrees from north in a clockwise direction)

2. The tool

In the following paragraph the framework of the GIS tool that was developed is summarized and the various criteria that were considered are presented. A digital map, which is a regular sampling over the territory of a value represented in the raster format (each pixel of the raster is the land unit) is considered for each criterion. The cell size is 100 m. The criteria that were taken into account can be divided into qualitative criteria and quantitative ones.

2.1. Qualitative criteria

Qualitative criteria are represented by means of Boolean operators applied on each cell of a raster map B (x,y). By means of a query the satisfaction, or not, of the considered condition can be checked. A value equal to 0 is assigned to the excluded land units (areas where PV plants cannot be placed) and a value equal to 1 is assigned to the included land units (areas where PV plants are admitted). The qualitative criteria that were considered, expressed as areas to be excluded, are:

- *Restricted areas*: built-up areas, lakes, rivers, mountains and other zones considered in regional planning instruments (like zones of rivers overflow).
- *Protected areas*: national and regional parks areas.
- *Land use capacity*: it is assessed using the standard international land use capacity classification into 9 classes (land use capacity system elaborated since 1961 by the Soil Conservation Service of the Department of Agriculture of the United States and adopted by the FAO in 1974). The better productive potential of the soil, referring to first, second and third classes was excluded. This function can be therefore written as

$$B_{lu}(x,y) = \begin{cases} 1 \;\; if \;\; lu(x,y) = 4\text{^},5\text{^},...9\text{^} \\ 0 \;\; if \;\; lu(x,y) = 1\text{^},2\text{^},3\text{^} \end{cases} \quad (1)$$

- *Sloped areas*: the slope $s(x,y)$ of the terrain affects both the optimal orientation and inclination of the sun catching surface and the technical feasibility of the solar plant. A limit value of slope form the technical point of view, was determined from a survey on various manufacturer and professionals, and was assumed equal to 15%. In fact,

above this slope, many specific constraints arise in both the construction and operation stages. This criterion can be therefore formalized as

$$B_s(x,y)=\begin{cases}1 \;\; if \;\; s(x,y)\le 15\% \\ 0 \;\; if \;\; s(x,y)>15\%\end{cases} \tag{2}$$

- *Geographical orientation*: the orientation $\gamma(x,y)$ of the land unit combines with the slope $s(x,y)$ of the land unit and influences the technical feasibility of the plant. In fact, for low slopes the orientation is irrelevant (it can be compensated by the support structures), instead, over steeper slopes, the orientation of the ground is a constraint that imposes that only south-oriented terrains can be considered. Some previous works can be found in literature [9], and the following conditions were fixed

$$B_\alpha(x,y)=\begin{cases}1 \;\; if \;\; s(x,y)\le 3\% \,, \forall\, \gamma(x,y) \\ 1 \;\; if \;\; 3\%<s(x,y)\le 15\% \,, 135<\gamma(x,y)<225 \\ 0 \;\; for\ all\ other\ cases\end{cases} \tag{3}$$

Given the variability of the considered data, it is evident that the digital geographical data collected are from different sources and with different scales and reference systems. Thus a firstly the reference system was homogenized to the UTM 32N WGS84.

Vector data (such as Restricted Areas, Protected Areas and Land Use Capacity that were obtained from the Environmental Geographical Information System Database of the Piedmont Region, www.sistemapiemonte.it /sitad) were converted to raster format with a rasterization cell size of 100 m.

The slope and orientation values for each land unit were calculated from a down-sampled release (100 m resolution) raster DTM which had an original cell size equal to 50 m.

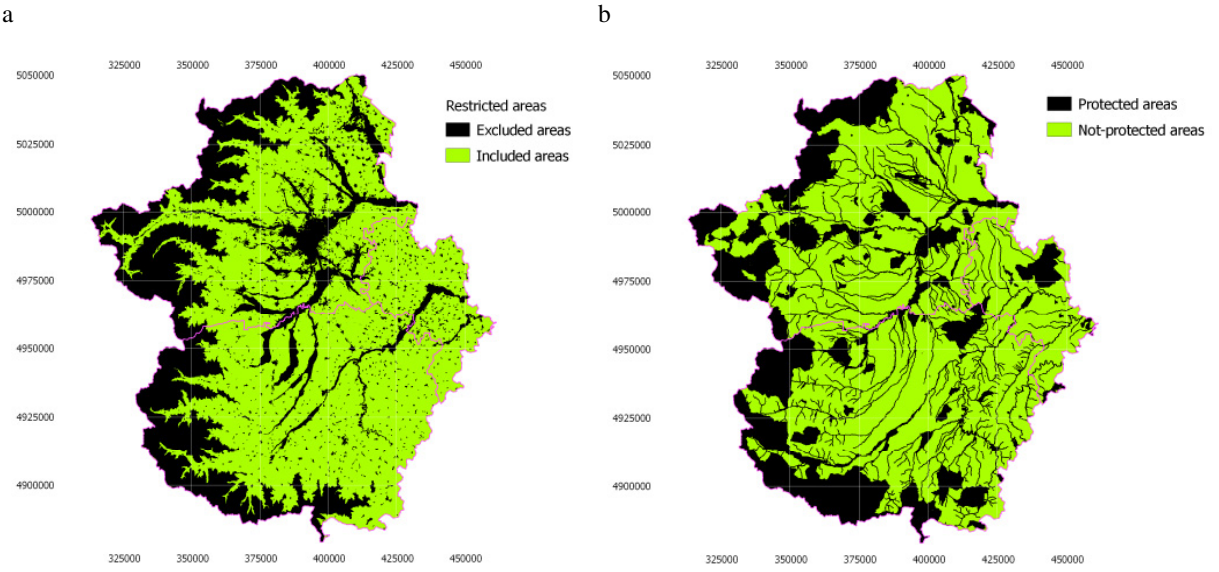

Fig. 1. (a) map of the restricted areas; (b) map of the protected areas.

The map of the previous criteria were determined and are reported in Figs. 1-2 where green pixels are representative of positive observations (value equal to 1) and vice versa for black pixels. It can be seen that the Restricted areas, Protected areas and Land use capacity criteria are not particularly stringent, however the Land use

capacity criterion tends to exclude all the areas that are placed in flat territory, while the Restricted and Protected areas are concentrated on mountain territory. The geographical orientation criterion reported in Fig. 2b is really stringent: only 10% of the total area is available. For the application of all the qualitative criteria see the Results paragraph (Fig. 5a).

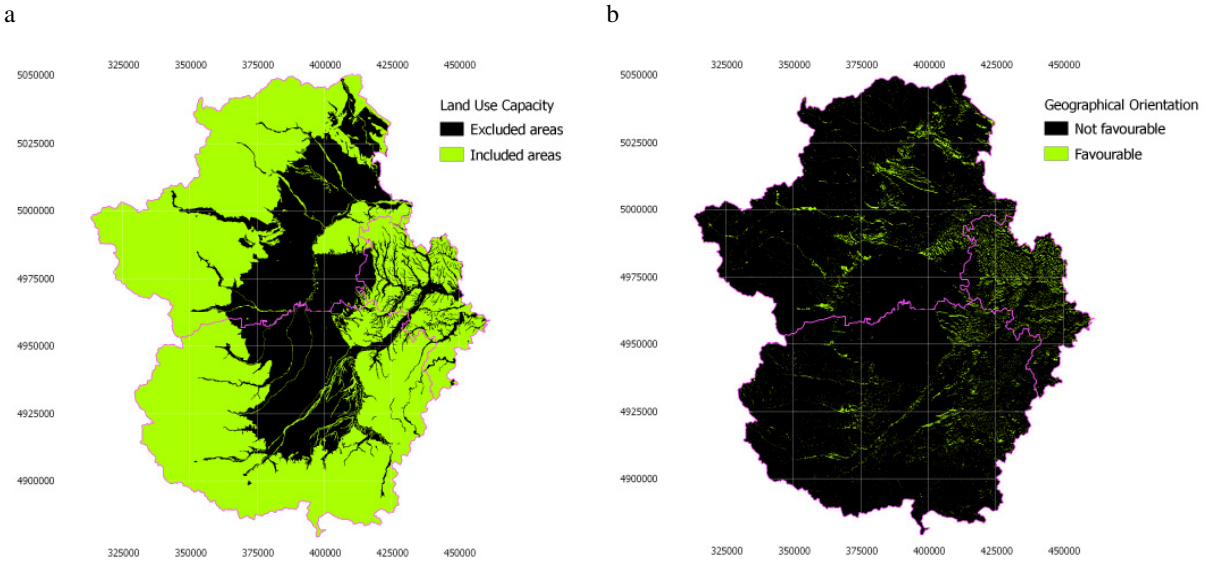

Fig. 2. (a) map of the land use criterion; (b) map of the geographical orientation criterion.

2.2. Quantitative criteria

Quantitative criteria are represented using raster representation of spatially distributed indices, $C_i(x,y)$, varying in the interval [0,1], for each pixel. A normalization, different for each criterion, is applied in order to constrain the index in the range [0,1]. For the solar radiation a criterion of maximum (the greater the solar radiation is, the most proximal to 1 is the indicator) was selected; the other two are criterion of minimum. These are:

- *Total annual solar radiation* (direct, diffuse and back-reflected from the ground) on horizontal plane. This quantity is necessary to have an indicator of the output (electricity or thermal) production of the plant. It was mapped using the routines available inside the ESRI ArcMap 9.3 GIS commercial software, however the input data of the standard routines were customized to obtain values which are consistent with the ones of the PV-GIS database [10] for some locations that were selected on the study area. The most important parameter that was modified was the ratio between diffuse and total radiation, and it was derived from the PV-GIS database for each of the four subset of DTM. The morphological features of the areas were determined on the basis of the available DTM. The DTM was partitioned into 4 different smaller DTM in order to allow a more refined calculation of the Sun position. The quantification criterion for this parameter (criterion of maximum) is expressed as

$$C_E(x,y)=\frac{\overline{C}_E(x,y)-\overline{C}_{E\min}}{\overline{C}_{E\max}-\overline{C}_{E\min}} \quad \text{where} \quad \overline{C}_E(x,y)=\frac{E(x,y)-\mu_E}{\sigma_E} \tag{4}$$

and $E(x,y)$ is the amount of the total annual solar radiation collected at the land unit. The value of $\overline{C}_{E\max}$ resulted equal to 2.461, and the value of $\overline{C}_{E\min}$ equal to 2.268, while the values of the mean (μ_E) and standard deviation (σ_E) resulting from the solar radiation map were respectively equal to 1584 kWh (mean value) and 185 kWh (standard

deviation value). In order to contain the index in the range [0,1] the two above mentioned normalizations (4) were applied, jointly permitting to minimize the negative effect of the outliers of the solar radiation map. Fig. 3a shows the correspondent map. Higher sun radiation values occur both for south oriented slopes, and for increasing height above sea increases.

- *Annual average air temperature*: this parameter takes into account the effect that the cooling of the module has on the improvement of the energy efficiency (criterion of minimum) as

$$C_t(x,y) = 1 - \frac{t(x,y) - t_{\min}}{t_{\max} - t_{\min}} \tag{5}$$

where $t(x,y)$ is the annual average air temperature, t_{min} the minimum temperature (– 3 °C) and t_{max} the maximum temperature (14.4 °C). Source data were provided in raster format with a cell size of 250 m from meteorological observations in a period of 17 years (1991-2007). Spatial interpolation was achieved by multivariate linear regression. Resulting map is reported in Fig. 3b.

- *Annual average rainfall cumulative height*: this parameter has to be considered an indirect indicator of soil aridity (criterion of minimum rainfall). Its role is to take care of the relationship between PV installations and agricultural production. From one side agriculture energy consumption can be reduced by sun energy exploitation, but, from the other side PV plants can subtract valuable soil for crop production [11].

$$C_h(x,y) = \frac{h_{min}}{h(x,y)} \tag{6}$$

where $h(x,y)$ is the annual average rainfall cumulative height and h_{min} is equal to 461 mm. Source data were provided in raster format with a cell size of 250 m from meteorological observations referring to a period of 17 years (1991-2007). Spatial interpolation was done using the spline method. Resulting map is reported in Fig. 4a.

a b

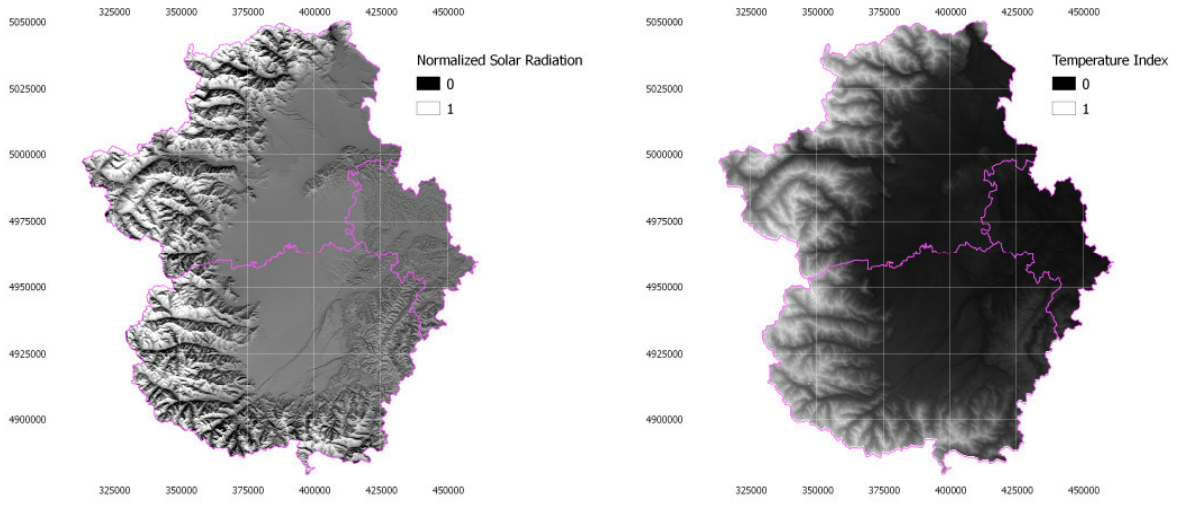

Fig. 3. (a) map of the normalized total annual solar radiation; (b) map of the annual average air temperature index.

2.3. Objective function and weights estimation

A synthetic index representing ground-mounted PV plants land carrying capability was defined by combining the above mentioned criteria according to (7).

$$f = \left(\sum_{i=1}^{n} \alpha_i \cdot C_i \right) \cdot \prod_{j=1}^{m} B_j \tag{7}$$

where n is the number of quantitative criteria $C(x,y)$, m is the number of qualitative criteria $B(x,y)$ and α_i are weights assigned to the quantitative criteria. Reasonable values for α_i were estimated by using an MLP (Multi Layer Perceptron) Artificial Neural Network (ANN). This approach was already used in literature for many applications as, for example, in [12,13]. ANN is a sort of self-structuring mathematical model approximating the relationship between some independent variables (ANN input) and a dependent one (output). The best architecture of the ANN, that is the best approximating relationship, is obtained through a training step achieved supplying to the ANN some reference observations (training set) for which both inputs and output are known. Assessment of the trained ANN parameters permits to obtain information concerning the relative weights of the inputs in the generation o the output.

20 already existing sites of PV plants in the Piedmont Region were recognized by photointerpretation from high resolution satellite images available from free WMS (Web Map Servers); they were used as positive reference set for ANN training; the correspondent values of C_E, C_t and C_h were extracted by the previously generated raster maps using the appropriate GIS tool. It is worth to stress the fact that not necessarily these parameters assume high values at the selected locations; nevertheless they were considered as representative of favourable sites for PV plants installation. To generate a negative reference set of observations, other 20 sites representative of the worst conditions were selected minimizing the parameters C_E, C_t and C_h.

The selected C_E, C_t and C_h values represent the ANN inputs; an arbitrary value varying in the range [0,1] was instead assigned to each set of inputs to represent the expected output. The assignation was done according to the following strategy. Values around 1.0 were assigned to observations selected as positive references; values around 0.0 were assigned to observations selected as the negative references. Values around 1.0 (O^+) were determined according to (eq. 8) and assigned to the 20 positive references; values around 0.0 (O^-)were determined according to (eq. 9) and assigned to the 20 negative references.

$$O_i^+ = 1.0 - [(C_{Ei}-1)^2+(C_{ti}-1)^2 +(C_{hi}-1)^2]^{0.5} \tag{8}$$

$$O_i^- = 0.0 + [(C_{Ei})^2+(C_{ti})^2 +(C_{hi})^2]^{0.5} \tag{9}$$

where (C_E=1, C_t=1, C_h=1) is the optimal reference and (C_E=1, C_t=1, C_h=1) the worst reference. C_{Ei}, C_{ti} and C_{hi} are the values of the generic input of the training set.

The better performing ANN architecture was determined by an iterative self-developed Matlab© routine [14,15] that tests different configurations of the ANN and it stops when a performance threshold (RMSE, Root Mean Squared Error of residuals) is reached. Table 1 reports parameters used during ANN training and structuring; Fig. 4b shows ANN final architecture.

Table 1. Training parameters and final architecture of the MLP ANN.

Training algorithm	*Back Propagation Levenberg-Marquardt*
N. of input nodes	*3*
N. of hidden nodes (trained ANN)	*4*
N. of output nodes	*1*
Hidden layer Transfer Function	*Symmetric sigmoid*
Output layer Transfer Function	*Pure linear*
N. of training epochs/configuration	*1200*

Performance Threshold (RMSE)	*0.001*
Minimum n. of nodes of the hidden layer	*2*

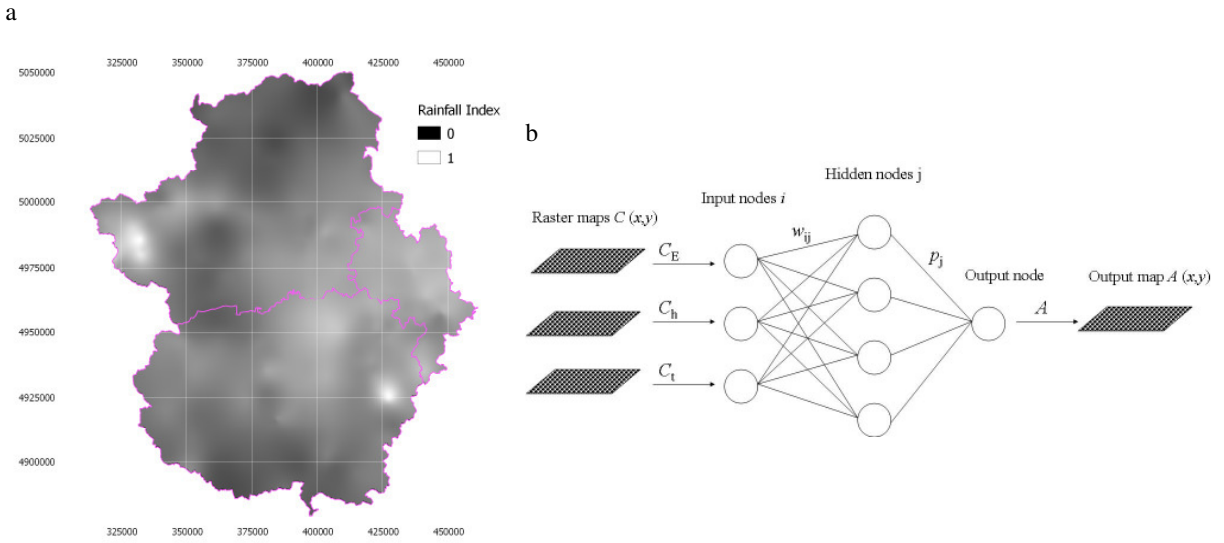

Fig. 4. (a) map of the annual average rainfall; (b) schematics of the ANN.

Final weights (w_{ij}) assigned to inputs (criteria) entering nodes of the hidden layer are reported in Table 2; weights (p_j) assigned to each hidden node entering the output layer are reported in Table 3. w_{ij} and p_j can be combined to estimate α_i to be assigned to the original criteria C_E, C_t and C_h (eq. 10).

$$\alpha_i = \sum_{j=1}^{4} w_{i,j} \cdot \frac{p_j}{100} \quad \forall \, i = \{1,2,3\} \tag{10}$$

where j is the number of hidden nodes. According to (10) α is equal to 62.47 % for C_E (solar radiation parameter), 6.96% for C_t (temperature parameter) and 30.57 % for C_h (rain parameter).

Table 2. Relative weights at the hidden layer of the trained ANN.

Hidden Layer	Weight C_E (i=1) (% at the node)	Weight C_t (i=2) (% at the node)	Weight C_h (i=3) (% at the node)	Total
Node j=1	88.71	3.61	7.68	100
Node j=2	43.74	12.90	43.36	100
Node j=3	41.85	5.19	52.96	100
Node j=4	60.51	8.55	30.94	100

Table 3. Relative weights at the output layer of the trained ANN.

Output layer	Node 1	Node 1	Node3	Node 4	Total
Weight (% at the node)	30.33	14.85	22.00	32.82	100

3. Results

Jointly considering all the inclusion/exclusion criteria (B_j in eq. 7) leads to a total available area representing less than 4% of the total one (Fig. 5a).

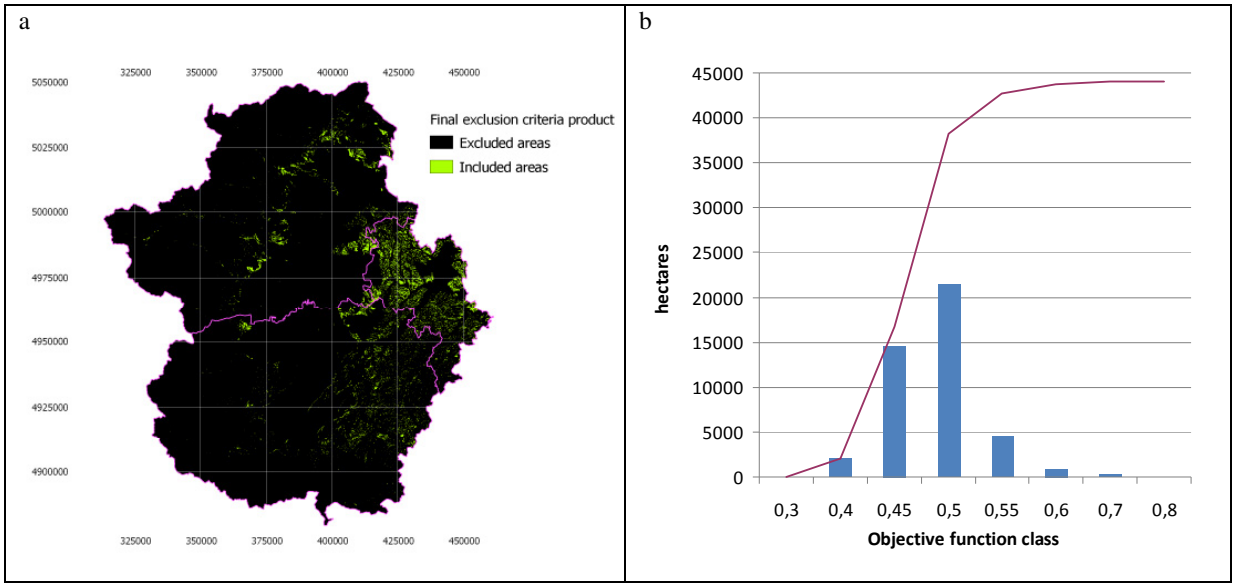

Fig. 5. (a) Map of areas admitting PV plant installation obtained by qualitative criteria product; (b) histogram of the objective function values.

Objective function (Fig. 6) was mapped using Eq. (7) by means of Raster Calculator tool available in ArcView 9.3. A first consideration that can be done is that areas that potentially admit PV plant installation are quite limited; furthermore they concentrate in the Asti and Cuneo provinces. 441 km² are potentially available; at these positions the objective function is higher than 0. The histogram representing the frequency distribution of the objective function values is shown in Fig. 5b; it is centered around classes 0.45 to 0.50.

Moreover if objective function map is more accurately assessed, it can be noticed that the most limiting factor is the one depending on the product of the qualitative exclusion/inclusion criteria; quantification criteria seem to not affect significantly the result, as the most of the objective function values falls in a very narrow range (0.45-0.55). Technological criteria instead appear to be much more stringent; in particular, the combination of the normative and technological criteria determines a strong reduction and a high fragmentation of the available areas (Fig. 5a).

To validate results, some sites were randomly selected and information given by the objective function map at those locations was compared with a higher scale technical cartography (1:10000 CTRN, Regional Map). The example that is reported in Fig. 7 shows a countryside site where land units (pixels) from the objective function map (100 m size) are overlaid onto the CTRN. Some discrepancies were observed in the randomly selected sites: for example, high values land units sometimes fall within villages where the restricted areas criterion should exclude their presence. Authors retain that this problem can be related to the use of a too low scale map (1:100.000) for the identification of built-up areas during the Restricted areas criterion definition. This map is quite approximate especially if farmsteads or small villages are present. Just large urban areas are considered. This observed limit can be useful to encourage once again users to operate integrating different geographic dataset and to always approach mapped functions obtained by modeling in a very critical way, possibly proceeding to detailed verifications for each project development.

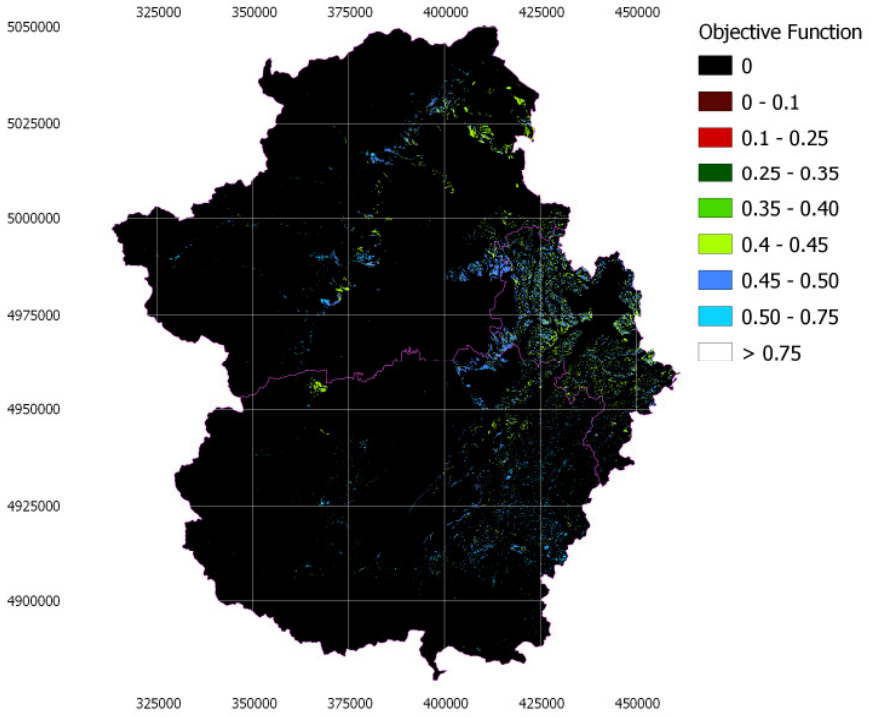

Fig. 6. Map of the objective function.

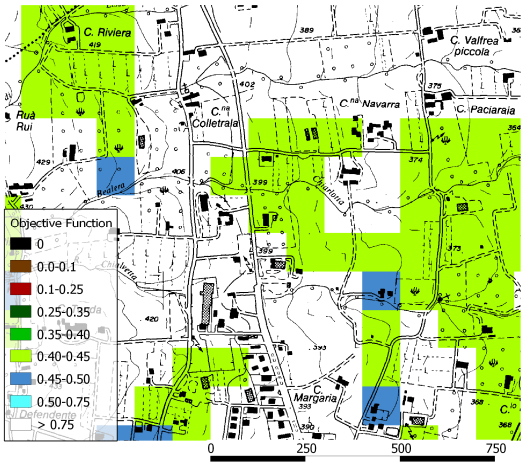

Fig. 7. Example of the objective function for a given site.

Discussing the application of the proposed methodology to solar thermal plants, it first can be noted that all the inclusion/exclusion qualitative criteria can be considered the same. Therefore, the significance of a map such as the one of Fig. 5a remains the same also for types of solar plants other than the PV ones. Passing to the quantitative criteria, the main difference between PV plants and solar thermal plants operations is due to the effect of the

temperature. In fact, a lower temperature is positive for PV installations because it has an increasing effect on the conversion efficiency of the PV module, while it is negative for solar collectors because it tends to decrease the collector instantaneous efficiency. This means that it should be represented in Eq. 5 as a criterion of maximum, instead of minimum. The other criteria remain the same. Once weighted with the weights determined by Eq. 8 , the effect of the temperature is the lower one (6,96 %), so this means that again the objective function representation of Fig. 6 can be considered representative, to a large extent, also of the results for solar thermal plants also. Further studies in order to refine the criteria of a best site analysis specifically tailored to solar thermal plants should however be conducted.

4. Conclusions

Exclusion criteria that were considered in this study and that are enforced by national or regional laws determine an important reduction of the areas potentially suitable for ground mounted PV plants. Just 441 km^2 (representing about 3% of the study area) were recognized as potentially devoted to host installations. This size give a potential of peak power of about 2900 MWp. Results can be retained of great interest for planners and energy managers at regional level. Even considering the most stringent requirements set by the regional governments to limit the installations, a considerable amount of available areas still exists.

Concerning the proposed methodology, authors retain that further investigations may refine the adopted criteria and, above all, those based on DTM. In particular height accuracy can probably heavily condition results. Newest Lidar (Light Detection and Ranging) data can provide more reliable information about this. It is worth to remind that, at this level, “suitability” does not necessarily mean “possibility”. Actual exploitation of suitable areas will be achieved only when appropriate landscape assessment will be made. Anyway, this has to be considered a second step of the analysis process to face only when all the various factors (e.g. an investor, financial income, etc.) converge to make the installation possible.

References

[1] Sørensen B. GIS management of solar resource data. Solar En Mat & Solar Cells 2001;67:503-9.
[2] Calvert K. Geomatics and bioenergy feasibility assessments: Taking stock and looking forward. Renew Sustain Energy Rev 2011;15:1117-24.
[3] Hossain J, Sinha V, Kishore, VVN. A GIS based assessment of potential for windfarms in India. Renew Sustain Energy Rev 2011;36:3257-67.
[4] Sliz-Szkliniarz B, Vogt J. GIS-based approach for the evaluation of wind energy potential: A case study for the Kujawsko–Pomorskie Voivodeship. Renew Sustain Energy Rev 2011;15:1696-707.
[5] Rogge E, Nevensa F, Gulinckb H. Reducing the visual impact of ‘greenhouse parks’ in rural landscapes. Landscape Urban Plann 2008;87:76-83.
[6] Domingo-Santos JM, Fernández de Villarán R, Rapp-Arrarás I, Corral-Pazos de Provens E. The visual exposure in forest and rural landscapes: An algorithm and a GIS tool. Landscape Urban Plann 2001;101:52-8.
[7] Chiabrando R, Fabrizio E, Garnero G. The territorial and landscape impacts of photovoltaic systems: definition of impacts and assessment of the glare risk. Renew Sustain Energy Rev 2009;13:2441-51.
[8] Chiabrando R, Fabrizio E, Garnero G. On the applicability of the visual impact assessment OAISPP tool to photovoltaic plants. Renew Sustain Energy Rev 2011;15: 845-50.
[9] Dominguez Bravo J, Garcia Casals X, Pinedo Pascua I. GIS approach to the definition of capacity and generation ceilings of renewable energy technologies. Energy Policy 2007;35:4879-92.
[10] Súri M, Huld T, Dunlop E. PV-GIS: a web-based solar radiation database for the calculation of PV potential in Europe. Int J Solar Energy 2005;24:55-67.
[11] Fabrizio E. Energy reduction measures in agricultural greenhouses heating: Envelope, systems and solar energy collection. Energy and Building 2012;53:57-63.
[11] Borgogno Mondino E, Gomarasca MA. FAMS: A Flooding Areas Monitoring System for early warning, Proceedings of 32nd International Symposium on Remote Sensing of Environment: Sustainable Development Through Global Earth Observations 2007Borgogno Mondino E,
[12] Ermini L, Catani F, Casagli N. Artificial Neural Networks applied to landslide susceptibility assessment. Geomorphology 2005;66:327–43.
[13] Lessio F, Borgogno Mondino E, Alma A. Spatial patterns of Scaphoideus titanus (Hemiptera: Cicadellidae): a geostatistical and neural network approach. Int J Pest Management 2011;57:205-16.
[14] Borgogno Mondino, E., Giardino M, Perotti L. A neural network method for analysis of hyperspectral imagery with application to the Cassas landslide (Susa Valley, NW-Italy). Geomorphology 2009;1-2:20-27
[15] Marquardt DW. An algorithm for least-squares estimation of nonlinear parameters. J Society Industrial Appl Mathematics 1944;11:431-41.